DENSITY BASED APPROACH FOR COLLISION RISK COMPUTATION

Francesca Letizia[(1)], **Camilla Colombo**[(2)], **and Hugh G. Lewis**[(3)]
[(1)(2)(3)]*University of Southampton, University Road, Southampton, SO17 1BJ, +442380593334, f.letizia@soton.ac.uk*

Abstract: *In February 2015 the satellite DMSP-F13 exploded in orbit producing 160 new trackable pieces of space debris. In the following days, operators assessed how the explosion affects the risk for their spacecraft, considering only debris objects larger than 10 cm. However, also smaller fragments are an important part of the debris population as any collision with objects larger than 1 mm may interfere with the spacecraft operation. The impact of a new fragmentation event considering also the presence of small fragments can be assessed by studying the fragment cloud in terms of its spatial density, applying the proposed method CiELO. Our formulation allows representing the long-term evolution of a large number of fragments with an analytical model based on the continuity equation. Moreover, it guarantees a limited computational effort compared to the standard approach of following each individual object. Once the cloud density is known, it is possible to build a collision map that identifies which are the most affected regions of space as a consequence of the breakup. Coupling this map with a database of spacecraft or space debris objects it is also possible to identify the most exposed targets. This kind of maps can be useful for operators to have a fast estimation of the increase in the long term collision risk on their missions.*

Keywords: *fragmentations, small debris fragments, collision probability*

1. Introduction

Space debris population collects all the non-functional man-made objects in orbit around the Earth. According to the Inter-Agency Space Debris Coordination Committee (IADC) [1], the majority (56.3%) of tracked space debris objects are *fragmentation* objects, that is objects generated by destructive events such as explosions and collisions. Historically, since 1961, 142 fragmentations occurred in Low Earth Orbit (LEO): a detailed description of each breakup occurred before 2003 can be retrieved from [2], whereas data on recent events can be derived from the analysis of the updates published on the Orbital Debris Quarterly News[1].

Figure 1 shows the distribution of the number of events and of the produced fragments with semi-major axis and inclination. It appears how the region between 700 and 900 km is the most affected by breakups, especially in the subset of sun-synchronous orbits (i.e. inclination between 90 and 100 degrees). This result can be explained considering that sun-synchronous orbits represent a highly exploited region of Space because of their advantageous point of view, with stable lighting conditions, for Earth observation missions. Moreover, at these altitudes (above 700 km) the effect of atmospheric drag becomes less and less effective. As atmospheric drag is the only available natural sink mechanism, breakups occurring at these altitudes are expected to generate fragments with a long orbital life-time, able to interfere for decades with the rest of the environment and with operational spacecraft.

This was the case for the two most important breakup occurred in LEO. The first one is the infamous Chinese anti-satellite test in 2007: a satellite, Fengyun-1C, with a mass of 880 kg,

[1]For the fragmentations described in the Orbital Debris Quarterly News the number of produced fragments was updated by checking `https://www.space-track.org`. Data retrieved between June and July 2015.

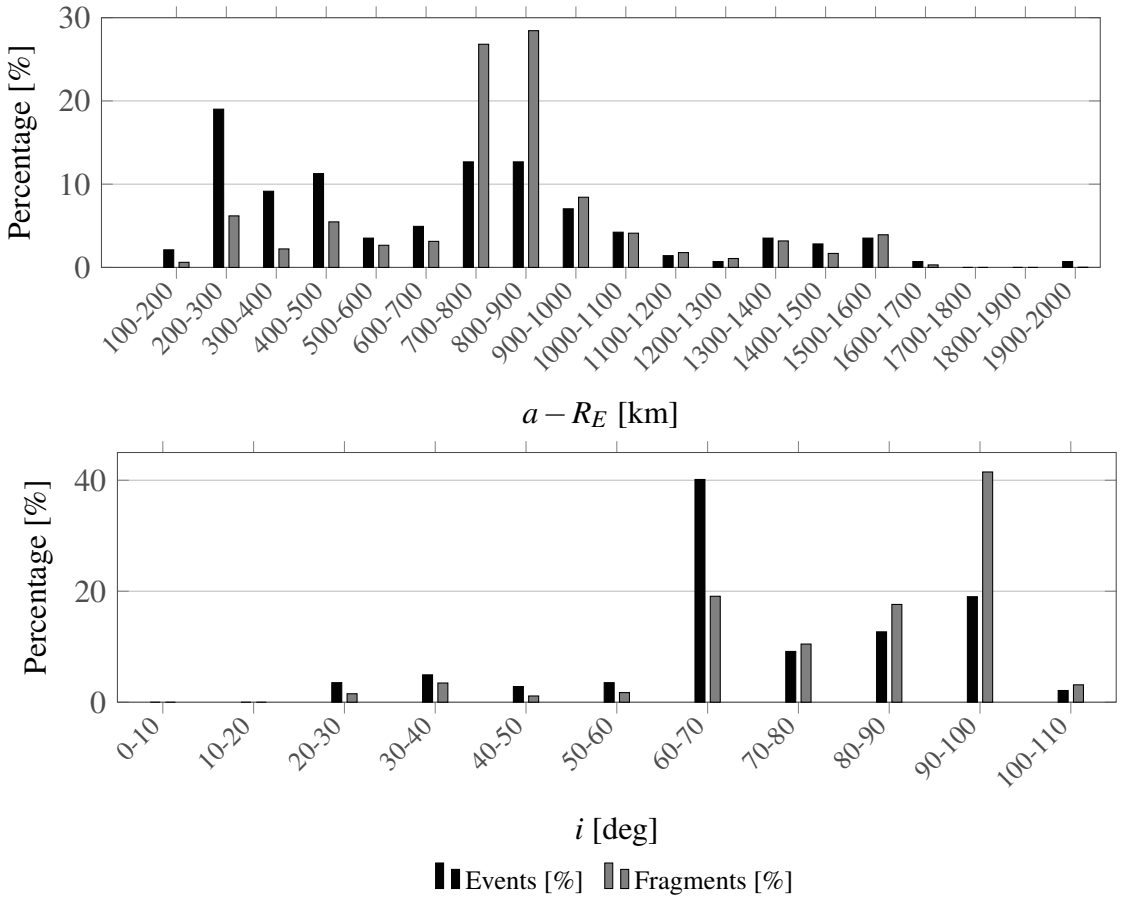

Figure 1: Distribution of events and number of generated fragments for the breakups in LEO in semi-major axis a and inclination i. The values are expressed as percentage of the total number of events (142) and fragments (16115).

was intentionally destroyed generating almost 2000 new catalogued objects, increasing of more than 60% the spatial density of objects at the fragmentation altitude (863 km) [3]. The second important event took place in 2009 and it is the collision between two satellites, Cosmos 2251 and Iridium 33, that generated more than 2000 new catalogued objects [4]. While Cosmos satellite was already non operational before the collision, Iridium 33 was still functioning, so in theory it could have manoeuvred to avoid the impact. Instead, it was manoeuvred, for operation purposes, in the direction of the abandoned spacecraft because the operators did not have accurate information on the position of Cosmos 2251 [5]. This shows how even when the location of space debris objects is known, the collision cannot always be avoided. Besides the event in 2009, other three collisions were documented between satellites and catalogued fragments [4]. In addition, since 2012, at least in six occasions, a collision between an uncatalogued piece of debris and a satellite was proposed as an explanation of satellite anomalies [6, 7, 8, 9]. These cases are an example of how also *small* (i.e. not trackable with radars) fragments affect the space environment. In fact, any object larger than 1 cm may be able to destroy a satellite in case of collision in LEO, whereas objects larger than 1 mm may interfere with the correct functioning of operational satellites [10, 11, 12]. For this reason, McKnight et al. [13] identify the so-called *lethal non-trackable* objects as the main threat to flight safety.

The major issue with fragmentation events is that their effect is not limited to the orbits where they happened, but rather they affect the global debris environment. For example, in March 2012, the six astronauts of the ISS sheltered in the Soyuz spacecraft as a precaution during a close passage of a fragment generated by the 2009 collision. More recently, on 27th October 2014, the ISS performed another manoeuvre to avoid a 8 cm fragment generated as well by the Cosmos-Iridium collision. This shows how important is to predict the motion of objects generated by a fragmentation event and evaluate they effect on the collision risk on the long term. In particular, operators may be interested in assessing, right after a breakup is detected, whether and how their spacecraft will be affected.

With this in mind, the aim of this work is to develop a tool that provides a quick estimation of the consequences of a fragmentation, identifying which spacecraft will be the most affected on the long term and which operators could expect an increased collision risk. This is achieved using an analytical propagator to describe the long term evolution of the density of the fragment cloud. The use of an analytical propagator allows including also small fragments in the risk assessment. In addition, thanks to our analytical approach and the formulation in terms of density, the analysis tool can be run on normal computers with a reasonable computational effort, with no request for supercomputing facilities. This means that, for example, the analysis can be easily repeated if new data on the fragmentation is available and that multiple collision scenarios can be studied.

The paper is organised as follows. Section 2 gives a brief description of the methods used to propagate the debris cloud and to compute the collision probability for an object crossing the cloud. Section 3 describes the tool developed to assess the fragmentation event. Section 4 show the application to a real fragmentation.

2. Propagation method

According to the NASA breakup model [14], for each trackable object produced by a fragmentation there are thousands objects in the size range between 1 mm and 5 cm. Considering

these numbers, even low intensity fragmentations can easily reach some thousands objects, whose individual propagation would make their simulation prohibitive in terms of computational resources (i.e. time and RAM). Evolutionary studies on the debris population usually deal with this issue by setting a cut-off fragment size at 10 cm, so that only objects larger than this threshold are included in the simulations. However, especially when the impact of a single breakup is analysed, it could be relevant to include all objects that are able to interfere with other spacecraft, reducing the threshold to 1 mm. This change in the scope of the analysis can be achieved by abandoning the evaluation of the single fragments' trajectories and studying the fragmentation cloud globally.

For this reason, the propagation method CiELO (debris Cloud Evolution in Low Orbits) was developed: within this approach, the fragmentation cloud is described in terms of its spatial density, whose evolution in time under the effect of drag is obtained by applying the continuity equation. A detailed description of the method can be found in [15], whereas only a brief overview of the approach is provided here, focussing mostly on the new improvements with respect to [15].

The simulation of a fragmentation event starts with the modelling of the breakup. The NASA breakup model [14] is used for this purpose. The evolution of the fragment cloud from this point is affected both by the dispersion of the energy among the fragments and the effect of perturbations. Considering only the case of fragmentations in LEO, the Earth's oblateness spreads the fragments to form a band around the Earth. Once the band is formed, the atmospheric drag can be considered as the main perturbation and the continuity equation can be applied to obtain the cloud density evolution, following the approach firstly proposed by McInnes [16].

Compared to McInnes' [16] formulation, where the debris density is function of the radial distance from the Earth (r) only, the method was extended to express the cloud density as function of semi-major axis (a) and eccentricity (e) [17]. This extension results into an increase in the method applicability: whereas the description with the distance only can be applied to orbits between 800 and 1000 km, the formulation in a and e can be used also for orbital altitudes between 700 and 800 km. This means that the analytical method can be employed for the whole region where the majority of fragmentations occurred (Fig. 1).

The fact that the continuity equation can be applied only once the band is formed means that alternative modelling techniques are required to describe the transition to the band. In [15] this was done by numerically propagating the trajectory of the fragments for the months required to form the band. In the new version of the model used in this work this is done by applying a method similar to the one embedded in the continuity equation, which does not involve integrating the fragments' trajectories. When the continuity equation is solved with the method of characteristics, the value of the solution at a certain time is obtained by *reshaping* the initial condition according to the change prescribed by the conservation of the solution along the characteristics. Similarly, modelling the first phase of the cloud evolution is equivalent to describe how the (a,e)-plane changes from the initial time of breakup to the time of band formation T_B to reproduce the evolution in Fig. 2.

The method based on the continuity equation is simplified by neglecting the variation of the eccentricity and only the variation of the semi-major axis a due to drag is considered. For each point in the a-axis it is possible to compute the variation of a in the time T_B and obtain

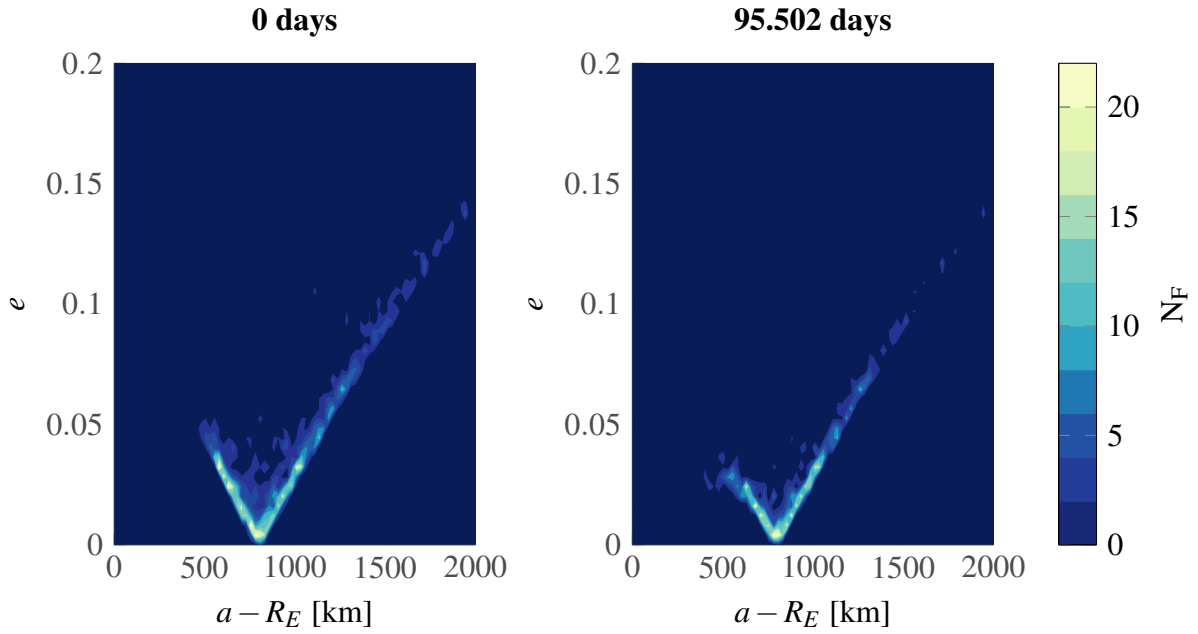

Figure 2: Visualisation of cloud density at the breakup and at the band formation T_B for a fragmentation at 800 km. N_F indicates the number of fragments.

a modified grid by applying the semi-analytical propagation method to evaluate the effect of drag [18]. Observe that the variation in a obviously depends on the area-to-mass ratio, so the computation should be repeated for each A/M bin in which the cloud is divided. It was shown that the optimal number is ten bins in A/M [15]. Once each value of the initial grid is mapped into its modified value, it is possible to obtain the distribution $n(a,e,T_B)$ from the initial one $n(a,e,0)$ with the following algorithm. Let a_j indicate the j-th point in the original grid and a_k its modified value after T_B; if $a_k < 0$ the fragments originally at a_j have re-entered and so $n(a,e,T_B)$ is not updated; if $a_k > 0$, $n(a_k,e,T_B) = n(a_j,e,0)$. In this way, the initial distribution $n_0(a,e)$ at the band formation is known.

This variation in the model is particularly important because removing completely the numerical propagation of the fragments' trajectory, also for a short phase as in [15], makes the computational effort of the model really independent on the number of fragments contained in the cloud. In this way, any breakup can be simulated with the same computational time. In addition, also large events can be simulated without supercomputer facilities as also the request of RAM is the fixed.

Once n_0 is known, the continuity equation can be used to obtain the long term evolution of the density n. The evolution of the fragment density in the space of orbital parameters is written as [17]

$$n(a,e,t) = n_0(a,e)\frac{v_a(a_i)}{v_a(a)} \tag{1}$$

where v_a is the rate of variation of the semi-major axis due to atmospheric drag. The expression of v_a is derived from King-Hele [19] and simplified in the following expression to solve the problem analytically

$$v_a(a) = -\sqrt{\mu_E R_F}\frac{c_D A}{M}\rho_0 \exp\left(-\frac{a-R_F}{H}\right) f(R_F, \tilde{e}a), H), \tag{2}$$

with μ_E gravitational constant of the Earth, R_F radial distance where the fragmentation occurred, c_D and A/M respectively drag coefficient and area-to-mass ratio of the fragments, ρ_0 and H atmospheric density and scale height at R_F. $\phi(R_F, \tilde{e}(a), H$ is a function that collects the Bessel functions, which describe the effect of eccentricity

$$f = I_0(z) + 2eI_1(z) + O(e^2) \tag{3}$$

where I_j is the Bessel function of the first kind and order j with argument $z = R_F\tilde{e}(a)/H$. The function $\tilde{e}(a)$ describes the initial distribution of eccentricity with semi-major axis. This means that the cloud is propagated with the (strong) assumption that the distribution of eccentricity with semi-major axis is constant through the whole simulation.

The value of the cloud spatial density is then obtained by applying expressions that allow expressing the probability of finding an object given its orbital parameters to the whole domain in (a, e). The expression used is [20, 21]

$$s(r) = \frac{1}{4\pi r a^2} \frac{1}{\sqrt{e^2 - \left(\frac{r}{a} - 1\right)^2}}, \tag{4}$$

where $s(r)$ indicates the density as a function of the radial distance.

It is important to highlight that the continuity equation is used to model only the density as a function of the geocentric distance, whereas the cloud density depends also on the latitude and this should be taken into account when assessing the collision probability for a spacecraft crossing the fragment cloud. Different authors [20, 21] have shown that the dependence on the distance r and on the latitude β can be described separately expressing the density as the product of two components:

$$S(r, \beta) = s(r)f(\beta). \tag{5}$$

This is particularly useful in the application to debris clouds as the evolution of the two parameters occurs with different time scales and drivers. In fact, the purpose of the proposed method is to study the long term (i.e. years) effect of a fragmentation, whereas the latitude of a target spacecraft crossing the cloud evolves in a much shorter time scale (i.e. hours). Following the target latitude would require very short time steps for the integration, eliminating or reducing the advantage of having a fast propagator for the fragment cloud. For this reason, an average value over β is considered. The average density value can be found computing once the integral average of $f(\beta)$ over one orbit period and apply it to rescale the spatial density at any time, recalling the hypothesis that the fragments' and the target's inclinations are not changing as the rotation of the Earth's atmosphere is neglected. The dependence of the latitude β on the orbital parameters is expressed by

$$\beta = \arcsin\left[\sin(\omega + \nu)\sin i\right] \tag{6}$$

where ω, ν, i refer to the argument of perigee, the true anomaly and the inclination of the target spacecraft crossing the cloud. Introducing the argument of latitude $u = \omega + \nu$ and writing the expression for the case of a target on a circular orbit, the scaling factor of the spatial density can be computed as

$$\bar{f} = \frac{1}{2\beta_{\max}} \int_0^{2\pi} \frac{\mathrm{d}u}{\sqrt{\cos^2(\beta(u)) - \cos^2(\beta_{\max})}} \tag{7}$$

where $\beta(u)$ is given by Eq. 6. $\beta_{\max}$ is the maximum latitude covered by the band. For non-equatorial orbits $\beta_{\max}$ is put equal to the inclination where the fragmentation occurred i_F if $i_F \leq \pi/2$ and equal to $\pi - i_f$ otherwise [22].

Once the cloud density at any time is known, it is possible to evaluate its effect on the collision probability for a spacecraft that crosses the cloud. The computation of the collision probability is based on the average number of collisions N in an interval of time [20]. This number is then used to obtain the cumulative collision probability for the target spacecraft through a Poisson distribution

$$p_c(t) = 1 - \exp(-N) \tag{8}$$

following the common analogy with the kinetic gas theory [23, 24]. the average number of collisions N in a given interval of time $\Delta t = t - t_0$ can be written as

$$N = F\sigma\Delta t \tag{9}$$

where F is the flux of particles and σ represents the collisional cross-sectional area [20]. This last parameter is usually defined considering the dimensions of both the colliding objects [20], but here only the target spacecraft area A_T is considered because the fragments are much smaller than it, so $\sigma \approx A_T$. The flux F is equal to

$$F = S(r,t)\Delta v \tag{10}$$

where $S(r,t)$ is the value of the spatial density obtained with the analytical method based on the continuity equation and applying the scaling factor due to the distribution in latitude. Δv is the average relative velocity between the targets and the fragments, which is also obtained from the orbital configuration of the target and the fragmentation [25]. In details,

$$\Delta v = \frac{\int\int \mathbf{I}(a,e)\mathbf{n}(a,e)\delta\mathbf{v}(a,e)\,dade}{\int\int \mathbf{I}(a,e)\mathbf{n}(a,e)\,dade} \tag{11}$$

with

$$\mathbf{I}(a_j,e_k) = 1 \quad \text{if } a_j(1-e_k) \leq r_T \leq a_j(1+e_k) \tag{12}$$

and $\mathbf{I}(a_j,e_k) = 0$ otherwise. In Eq. 11, δv indicates the estimated relative velocity between the target and the points in the (a,e)-plane where n is evaluated

$$\delta v = \frac{2}{\pi}\sqrt{\chi+\eta}\,\mathrm{E}\left[\frac{2\eta}{\chi+\eta}\right] \tag{13}$$

with E complete elliptic integral of the second kind and

$$\begin{aligned}\chi &= v_T^2 + v_F^2 - 2v_T v_F \cos\gamma_F \cos i_T \cos i_F \\ \eta &= 2v_T v_F \cos\gamma_F \sin i_T \sin i_F,\end{aligned}$$

where

$$v_F = \sqrt{2\mu\left(\frac{1}{r_T} - \frac{1}{2a_F}\right)} \quad \cos^2\gamma_F = \frac{a_F(1-e_F^2)}{r_T(2a_F-1)};$$

the subscripts F and T refers to quantity of the fragments and of the target respectively.

3. Fragmentation analysis

The simulation of the fragmentation starts from the estimation of the input parameters required by the NASA breakup model, which are the kind of event (i.e. explosion, non-catastrophic collision, catastrophic collision), the class of object involved in the breakup, and the level of

energy of the event. The first parameters are usually known as, when new objects are observed, their origin is often identified. The kind of fragmentation can be determined considering that explosions and collisions result in a different distribution of energy. Explosions tend to produce larger fragments with lower speed compared to collisions. Finally, the energy level of the event can be estimated knowing the number of objects added to the catalogue and assuming that they are larger then a threshold value (e.g. 5 cm). In the case of an explosion no further information is required, whereas for collision also the impact velocity needs to be estimated or otherwise an average value is used. In the current implementation, an average collision velocity equal to 10 km/s is used. The event is replicated producing all the fragments down to 1 mm. To identify which regions of space are the most affected by a given fragmentation, a grid in semi-major axis and inclination is defined. Each cell defines a fictitious spacecraft with given semi-major axis and inclination, for which the collision probability with the fragment cloud is computed. Average values for the spacecraft area and mass are used to describe its trajectory evolution. These values were computed starting from a list of satellites available online [26], filtered to keep only spacecraft with perigee and apogee between 700 and 1000 km and mass larger than 50 kg. The resulting values are $A_T = 11\,\mathrm{m}^2$ and $M_T = 2322\,\mathrm{kg}$.

The collision probability is computed starting from the moment when the fragment cloud is spread around the Earth forming a band. The resulting cumulative collision probability at the end of the time window is the plotted as a function of the semi-major axis and the inclination to highlight which orbital regimes are the most affected. This graph is indicated as the *effect map*. The resulting *map* can be coupled with a database of spacecraft or space debris objects, such as the one in [26], to identify which are the most exposed targets. The idea here is not to propagate all the possible targets, but rather to use the information in the produced *effect map*. This can be done defining an index of *exposure* (η) and assigned it to all the spacecraft in the database. The index here used is composed of two elements: first, the value of the cumulative collision probability, obtained from the *effect map*, at the nominal orbit of the satellite; second, the mass of the satellite, taken as an indirect measure of the target cross-sectional area. The index is obviously an approximation because it does not consider the variation of the orbit during the years when the cumulative collision probability is computed; moreover, it implicitly assumes that all the spacecraft have the same area-to-mass ratio A/M. Nevertheless, it can give a first indication on which satellites are the most affected by a fragmentation event and then the result can be refined studying the collision probability for each target.

The index η for a spacecraft j is computed as

$$\eta_j = 1 - \left[1 - \mathbf{p_c}(a_j, i_j)\right]^{\frac{M_j}{M_T}}$$

where a_j, i_j are its semi-major axis and inclination; $\mathbf{p_c}$ is the map of collision probability in the *effect map*, so $\mathbf{p_c}(a_j, i_j)$ is the value for the spacecraft nominal orbit; M_j is the satellite mass and M_T is the reference value used to obtain $\mathbf{p_c}$. This expression for η was chosen because it can be related to the cumulative collision probability for the studied spacecraft. In fact,

$$\begin{aligned} 1 - \eta &= \left[1 - \mathbf{p_c}(a_j, i_j)\right]^{\frac{M_j}{M_T}} \\ \log(1 - \eta) &= \frac{M_j}{M_T} \log\left[1 - \mathbf{p_c}(a_j, i_j)\right]; \end{aligned}$$

for a Poisson process $1 - p_c = \exp(-N)$, so

$$1 - \eta = \left[1 - \mathbf{p_c}(a_j, i_j)\right] \exp\left(\frac{M_j}{M_T}\right) = \exp(-N) \exp\left(\frac{M_j}{M_T}\right)$$

and given the expression for N

$$1 - \eta = \exp\left(-n\Delta v \sigma \Delta t \frac{M_j}{M_T}\right). \tag{14}$$

Rewriting σ as

$$\sigma = \frac{A_T}{M_T} M_T$$

Equation 14 becomes

$$1 - \eta = \exp\left(-n\Delta v \Delta t \frac{A_T}{M_T} \frac{M_T}{M_T} M_j\right)$$

and using the assumption that A/M is the same for all the satellites

$$1 - \eta = \exp\left(-n\Delta v \sigma_j \Delta t\right) \quad \Rightarrow \quad \eta = 1 - \exp\left(-n\Delta v \sigma_j \Delta t\right) \approx p_{c,j}. \tag{15}$$

It is important to underline that Equation 15 is not the exact collision probability for the spacecraft j because the effect of the different values of the satellite area and mass on the trajectory evolution are not considered.

4. Application to DMSP-F13

The method was applied to study the fragmentation of the satellite DMSP-F13 occurred in February 2015. As a result of the event, probably due to a malfunctioning of a battery, 160 new objects were added to the catalogued[2]. At the moment of fragmentation, the spacecraft was in an orbit with an altitude between 844 and 856 km, with inclination equal to 98.8 degrees.

Assuming the objects to be larger than 5 cm and applying the equations of the NASA breakup model for explosions, 83598 fragments larger than 1 mm are expected. In fact, according to the NASA breakup model [14], the distribution of fragments with size is given by

$$N_f = 6 S L_c^{-1.6}, \tag{16}$$

where N_f indicates the number of fragments larger than the characteristic length L_c. S is a dimensionless parameter that depends on the exploding body. This parameter can be used to *tune* the explosion, so that setting L_c equal to 5 cm, N_f is equal to the number of new observed objects (i.e. 160). In this way, $S = 0.221$ is obtained. Applying again Eq. 16 with $S = 0.221$ and $L_c = 1$ mm, $N_f = 83598$ is obtained. The estimated total mas of the fragments is equal to 8.17 kg, so compatible with the explosion of a battery.

The first analysis we propose looks at the evolution of the cloud density with time. A time window of 15 years was used in this application. Figure 3a shows the evolution of the cloud spatial density with time, allowing for an estimation of which altitudes are the most affected at

[2]Data retrieved from `https://www.space-track.org` on 14 September 2015

different epochs. Observe that, according to the model, the highest object density at each altitude is observed at the beginning of the simulation. The density peak moves towards lower altitudes than the initial one, but the its absolute value is always lower than the value of the density at the band formation at that altitude. Figure 3b shows the cloud density normalised by the density of the background population. This is extracted from ESA MASTER 2009 including all objects larger than 1 mm. This plot can be useful to size the expected additional risk compared to the scenario without the breakup.

Table 1: Top affected spacecraft for the explosion of DMSP-F13 from the database in [26].

Spacecraft	SATCAT	a [km]	i [deg]	m [kg]	η
USA-144	25744	800	63.4	18000	0.044150
USA-182	28646	714.5	57.01	14500	0.021326
MetOp-A	29499	820.5	98.7	4193	0.016808
Persona-2	39177	723.5	98.3	7000	0.016794
MetOp-B	38771	820.5	98.7	4085	0.016379
Spot 5	27421	825	98.6	3030	0.012175
Radarsat-2	32382	792	98.6	2924	0.011876
Meteor-M2	40069	823.5	98.81	2778	0.011168
Meteor-M	35865	819	98.6	2700	0.010856
Worldview 2	35946	766	98.5	2800	0.010201

The analysis of the effect of the breakup on the different orbital regimes is shown in Fig. 4. It presents the *effect* map described in Sec. 3 considering 15 years of the cloud evolution. Figure 4 clearly shows that the most affected regions are the ones with altitude slightly lower than the one where the explosions occurred and with inclination i such that $\sin i \approx \sin i_F$, with $i_F = 98.8$ degrees inclination of DMSP-F13. With this orbital configuration, the target spacecraft crosses the cloud at the extremes of the band, where the density is maximum. The orbits within 50 km below the fragmentation appear to be affected for any value of their inclination: as the fragmentation occurred at 98.8 degrees of inclination, the band extends up to 81.2 degrees in latitude. This means that all objects with i such that $\sin i \leq \sin i_F$ will spend their whole orbits within the fragment cloud. On the other hand, objects with $\sin i > \sin i_F$ will spend a portion of their orbits outside the fragment band. This explains why in Fig. 4 the collision probability is lower for orbits with $i = 90$ degrees than for the adjacent values of inclination. The collision probability is still higher for $i = 90$ degrees than for $i = 70$ degrees because in the first case the target crosses the latitudes with the highest fragment density.

Figure 4 shows also the ten most affected spacecraft as extracted from the database in [26]. The spacecraft are indicated in Fig. 4 with a marker whose colour is related to the spacecraft exposure η, with the darkest markers associated with the highest values of η. The value of η for each spacecraft and their semi-major axis, inclination, and mass are reported in Tab. 1. For the top two spacecraft (USA-144 and USA-182), the dominant factor is the mass as these spacecraft have a mast at least double than any other object in the list. It is important to highlight that both satellites belong to classified projects by the United States National Reconnaissance Office[3], meaning that two-line elements are not available and their parameters (both orbital and physical) are deducted by the observations of amateur satellite observers. For this reason, the

[3]NASA National Space Science Data Center, `http://nssdc.gsfc.nasa.gov/`, last access 25 September 2015.

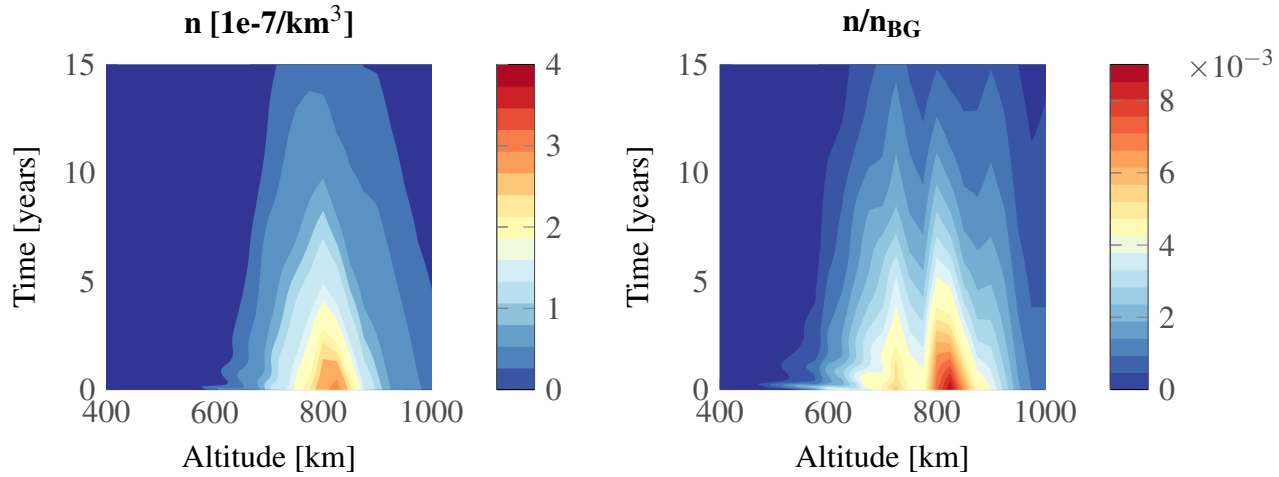

(a) Absolute value (b) Ratio compared to background density

Figure 3: Visualisation of cloud density evolution for the fragmentation of DMSP-F13.

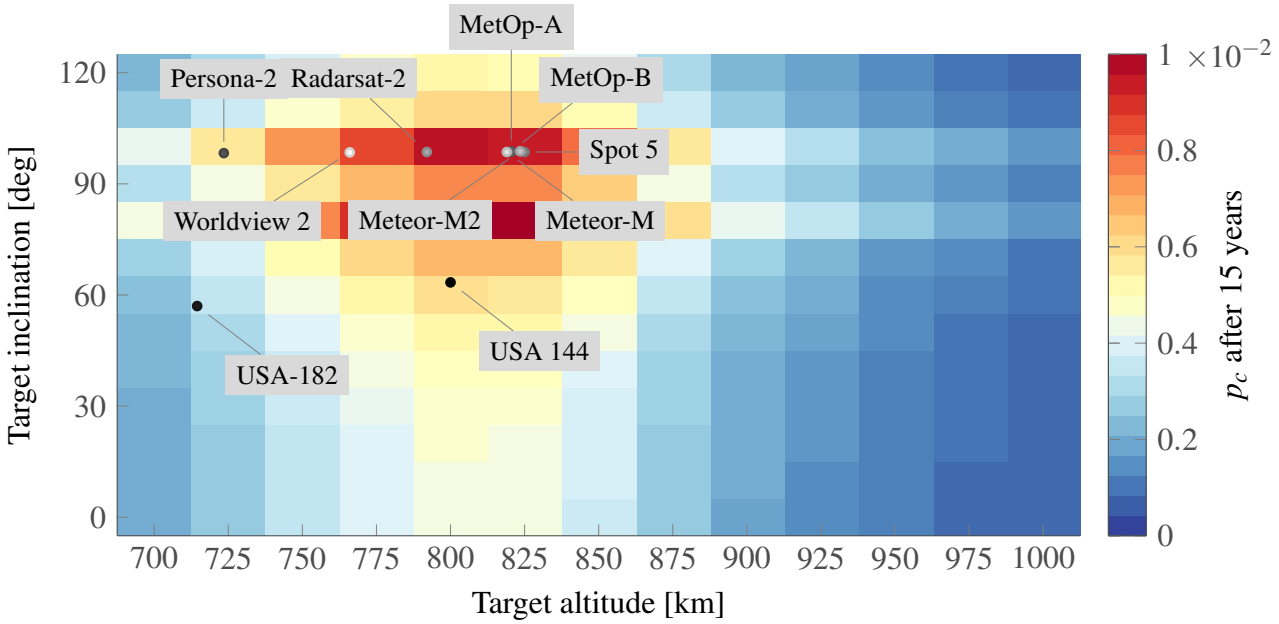

Figure 4: Effect map and top affected spacecraft for the explosion of DMSP-F13 from the database in [26].

reliability of the data on these satellites is much lower than the other ones in the list. In any case, as in this work the main focus is on the description a method to analyse a fragmentation, these spacecraft were kept in the database, using the values provided in [26]. Within the hypotheses of the proposed approach, high mass translates into high cross-sectional area, so USA-144 and USA-182 dominates the η rank even if their orbits are not in the regions most affected by the fragmentation. For the other spacecraft in Tab. 1, the orbit parameters play a major role. For example, MetOp-A presents a higher value of η than Persona-2 even if its mass is much lower (4193 kg versus 7000 kg) because its orbits lies in one of the regions with the highest cumulative collision probability.

The approach was tested also with a different satellite database, DISCOS[4] [27], Database and Information System Characterising Objects in Space, maintained by ESA. Also in this case, the database[5] was pre-filtered to keep only spacecraft with perigee higher than 700 km, apogee lower than 1000 km, mass larger than 900 kg. In addition, only spacecraft launched in the past ten years are considered, assuming that this threshold can be used to study only active satellites. Observe that this criterion removes Spot 5 from the database as it was launched in 2002, whereas includes Persona-1 that was launched in 2008, but failed some months after the launch. For the reasons already mentioned, USA-144 and USA-182 are not present in DISCOS. Besides these differences in the database, Fig. 5 and Tab. 2 show coherent results with the previous database. Observe that the *effect* map in Fig. 5 is not exactly the same as in Fig. 4 as different runs of the breakup model were used. The results appear robust to this variation, with similar ranking in Tab. 1 and Tab. 2. In Tab. 2, as the spacecraft have more similar masses than the one in Tab. 1, the combined effect of mass, semi-major axis, and inclination can be better appreciated. Eight out of ten spacecraft have inclination very close to the one of DMSP-F13, so this parameter appears extremely relevant in identifying the most affected spacecraft. Observe also from Tab. 2 how analysing only the spacecraft features does not allow deriving directly how affected each spacecraft is or ranking them. The proposed method enables the translation of qualitative statements (e.g. spacecraft with altitude closer to the fragmentation one are highly affected) into a quantitative assessment of the risk for any object.

It is also important to highlight that DISCOS actually contains information on the objects' cross-sectional area: this value could be used to remove the hypothesis that all objects have the area-to-mass ratio and obtain more reliable results. Future work will investigate this option. For the moment, it was preferred to develop a tool that can be easily used by any operator exploiting the availability of a database such as the one in [26].

For this reason, it is also important to briefly discuss the software structure and its computational requirements. All the code is currently written in MATLAB and it reads an input file with data on fragmentations (i.e. the orbital parameters of the fragmenting objects, the number of new detected objects, the class of breakup). The user then selects which case to simulate, the length of the simulated period (e.g. 15 years), the requested output and if the top affected spacecraft should be identified. In this case, also the name of the file containing the database with potential targets should be provided. A run starts with the simulation breakup and the propagation of the cloud density; the collision probability for each synthetic target is computed and, finally, if requested, the analysis of the target database is performed. Intermediate files are saved after the cloud propagation and after the computation of the collision probability, so that, respectively,

[4] `https://discosweb.esoc.esa.int`

[5] Data retrieved on 17 June 2015

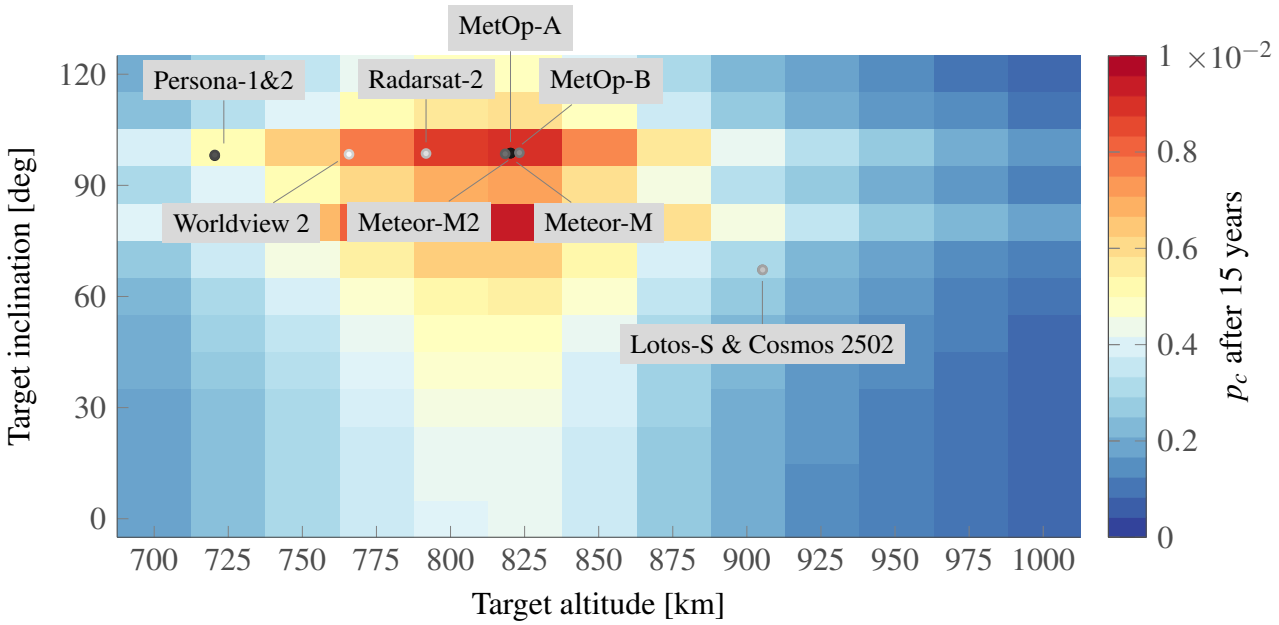

Figure 5: Effect map and top affected spacecraft for the explosion of DMSP-F13 from DISCOS database.

Table 2: Top affected spacecraft for the explosion of DMSP-F13 from DISCOS database.

Spacecraft	SATCAT	a [km]	i [deg]	m [kg]	η
MetOp-A	29499	820.24	98.7	4086	0.009357
MetOp-B	38771	820.34	98.7	4086	0.009357
Persona-1	33272	720.44	98	7000	0.009163
Persona-2	39177	720.44	98.2	7000	0.009163
Meteor-M	35865	818.44	98.5	2755	0.006319
Meteor-M2	40069	823.24	98.8	2755	0.006319
Lotos-S	36095	905.24	67.2	7000	0.005421
Cosmos 2502	40358	905.34	67.2	7000	0.005421
Radarsat 2	32382	791.74	98.6	2300	0.005199
Wordlview 2	35946	765.74	98.4	2615	0.005178

analyses with different grids of the *effect* map and with different target database can be performed without re-running the whole simulation.

The computational time for a complete simulation is equal to 9.52 minutes on a machine with 4 CPU at 3.40 GH and with 16 GB of RAM. Out of the total time, 5 minutes are spent for the cloud generation and propagation, 4.28 minutes for the computation of the collision probability, 5.24 seconds for the analysis of the target database.[6] These computational times allows for a quick assessment of fragmentations in Low Earth Orbits and are compatible with frequent runs in case of updates on the fragmentation data or on the target list.

5. Conclusions

As the number of debris objects increases, new challenges for operators arise. Considering that any object larger than 1 mm is able to cause anomalies in the functioning of a satellite, studying the trajectory of all objects that can interfere with operational spacecraft appears not feasible without the use of supercomputers. For this reason, a novel propagation method, CiELO, based on the description of the debris spatial density, was developed. According to the proposed approach, the fragment cloud produced by a breakup is described considering the evolution of its spatial density with time. Only the effect of atmospheric drag is considered, so that an analytical expression for the spatial density is possible. The analytical propagation method is coupled with an analytical estimation of the the average relative velocity between the fragments in the cloud and an object crossing the cloud. This allows for a quick estimation of the collision probability for any object crossing the fragment cloud.

The model was applied to develop a modular to assess the consequences of a breakup. The tool is able to determine which regions of space are the most affected by a fragmentation by representing each region with a synthetic target. The cumulative collision probability for each target is computed to obtain the so-called *effect* map, a representation of the total cumulative collision probability after the simulation period (i.e. 15 years) as a function of semi-major axis and inclination. Coupling this map with a list of potential target (e.g. active satellites), also the most affected spacecraft can be identified.

The case of the explosion of DMSP-F13 was studied in detail. The breakup, occurred in February 2015, produced 160 new trackable objects that, according to the NASA breakup model, suggest the presence of more than 80 000 objects larger than 1 mm. The spatial density of the resulting fragment cloud was studied for 15 years. According to the model, the most affected orbits are the ones with altitude within 50 km below the fragmentation one and the orbits with inclination i such that $\sin i \approx \sin i_F$, with i_F inclination of DMSP-F13. It was explained how this result is related to the distribution of the fragments with latitude across the cloud. As the cloud density is maximum at the band extremes, spacecraft that cross these regions will be the ones with the highest collision probability. This was also confirmed by the lists of the most impacted spacecraft. These lists were obtained from a database of active spacecraft free available online and from the ESA DISCOS database, finding consistent results. It was also shown how the proposed method allows quantifying the spacecraft exposure to the fragmentation considering the concurrent effect of mass, semi-major axis, and inclination. The analysis of a fragmentation requires less than ten minutes on a normal PC, enabling repeated analysis in case of variations in the breakup data (e.g. number of new observed fragments) or in the target list.

[6] All the computational times include the time to save the related output files.

6. Acknowledgements

Francesca Letizia would like to thank the DLR for the support received to attend the 25th International Symposium on Space Flight Dynamics. The authors would like also to thank Stijn Lemmens for the support with DISCOS and Dr. Holger Krag for the feedback on the application of the method. ESA MASTER 2009 was used as the reference debris population.

7. References

[1] IADC. "Space Debris: IADC Assessment Report for 2011." Iadc-12-06, Inter-Agency Space Debris Coordination Committee, Apr. 2013. [Online] Retrieved on 18/03/2015.

[2] Orbital Debris Program Office. "History of on-orbits satellite fragmentations.", May 2014. [Online] Retrieved on 26/08/2015.

[3] Pardini, C. and Anselmo, L. "Evolution of the debris cloud generated by the Fengyun-1C fragmentation event." NASA Space Flight Dynamics Symposium, pp. 1–13, 2007.

[4] Pardini, C. and Anselmo, L. "Review of past on-orbit collisions among cataloged objects and examination of the catastrophic fragmentation concept." Acta Astronautica, Vol. 100, pp. 30–39, Aug. 2014. doi:10.1016/j.actaastro.2014.03.013.

[5] Pardini, C. and Anselmo, L. "Physical properties and long-term evolution of the debris clouds produced by two catastrophic collisions in Earth orbit." Advances in Space Research, Vol. 48, No. 3, pp. 557–569, Aug. 2011. ISSN 02731177. doi:10.1016/j.asr.2011.04.006.

[6] NASA Orbital Debris Program Office. "Iridium Anomalous Debris Events." Orbital Debris Quaterly News, Vol. 16, No. 1, pp. 1–2, 2012.

[7] NASA Orbital Debris Program Office. "Two Derelict NOAA Satellites Experience Anomalous Events." Orbital Debris Quaterly News, Vol. 16, No. 1, pp. 1–2, 2012.

[8] NASA Orbital Debris Program Office. "Small Satellite Possibly Hit by Even Smaller Object." Orbital Debris Quaterly News, Vol. 17, No. 2, p. 1, 2013.

[9] NASA Orbital Debris Program Office. "A New Collision in Space?" Orbital Debris Quaterly News, Vol. 19, No. 1, p. 2, 2015.

[10] Krisko, P. H. "The predicted growth of the low-Earth orbit space debris environment an assessment of future risk for spacecraft." Proceedings of the Institution of Mechanical Engineers, Part G: Journal of Aerospace Engineering, Vol. 221, No. 6, pp. 975–985, Jan. 2007. doi:10.1243/09544100JAERO192.

[11] McKnight, D. S. and Di Pentino, F. "Semi-Empirical Satellite Anomalies Analysis Highlighting Contributions from the Fengyun-1C Event." "64th International Astronautical Congress," (International Astronautical Federation, Paris, France, 2013), Sep. 2013. IAC-13.A6.2.1.

[12] Wiedemann, C., Kebschull, C., Flegel, S. K., Gelhaus, J., Möckel, M., Braun, V., Radtke, J., Retat, I., Bischof, B., and Voersmann, P. "On-orbit fragmentation of Briz-M." "64th International Astronautical Congress," (International Astronautical Federation, Paris, France, 2013), Sep. 2013. IAC-13.A6.2.2.

[13] McKnight, D. S., Di Pentino, F. R., and Knowles, S. "Massive collisions in LEO – A catalyst to initiate ADR." "65th International Astronautical Congress," (International Astronautical Federation, 2014), Sep. 2014. ISSN 1995-6258. IAC-14-A.6.2.1.

[14] Krisko, P. H. "Proper Implementation of the 1998 NASA Breakup Model." Orbital Debris Quarterly News, Vol. 15, No. 4, pp. 1–10, 2011.

[15] Letizia, F., Colombo, C., and Lewis, H. G. "Analytical model for the propagation of small debris objects clouds after fragmentations." Journal of Guidance, Control, and Dynamics, Vol. 38, No. 8, pp. 1478–1491, 2015. doi:10.2514/1.G000695.

[16] McInnes, C. R. "An analytical model for the catastrophic production of orbital debris." ESA Journal, Vol. 17, No. 4, pp. 293–305, 1993.

[17] Letizia, F., Colombo, C., and Lewis, H. G. "Continuity equation method for debris cloud evolution.", 2014. Submitted to *Advances in Space Research*.

[18] Colombo, C. "Semi-analytical propagation for highly elliptical orbits to build maps for end-of-life disposal." "International workshop on Key Topics in Orbit Propagation Applied to Space Situational Awareness," (Logroño, 2014), Apr. 2014.

[19] King-Hele, D. Satellite orbits in an atmosphere: theory and application (Blackie, Glasgow and London, 1987), 1987. ISBN 0216922526.

[20] Kessler, D. J. "Derivation of the collision probability between orbiting objects: the lifetimes of Jupiter's outer moons." Icarus, Vol. 48, No. 1, pp. 39–48, Oct. 1981. doi:10.1016/0019-1035(81)90151-2.

[21] Sykes, M. "Zodiacal dust bands: Their relation to asteroid families." Icarus, Vol. 9, 1990.

[22] Letizia, F., Colombo, C., and Lewis, H. G. "Collision probability due to space debris clouds through a continuum approach." Journal of Guidance, Control, and Dynamics, 2015. doi:10.2514/1.G001382. Accessed on September 10, 2015.

[23] McKnight, D. S. "A phased approach to collision hazard analysis." Advances in Space Research, Vol. 10, No. 3-4, pp. 385–388, Jan. 1990. doi:10.1016/0273-1177(90)90374-9.

[24] Su, S.-Y. and Kessler, D. "Contribution of explosion and future collision fragments to the orbital debris environment." Advances in Space Research, Vol. 5, No. 2, pp. 25–34, Jan. 1985. doi:10.1016/0273-1177(85)90384-9.

[25] Letizia, F., Colombo, C., and Lewis, H. G. "2D continuity equation method for space debris cloud collision analysis." "25th AAS/AIAA Space Flight Mechanics Meeting," (AAS/AIAA, 2015), Jan. 2015. AAS 15-293.

[26] Union of Concerned Scientists. "Satellite Database.", Jul. 2014. [Online] Retrieved on 04/03/2015.

[27] Flohrer, T., Lemmens, S., Bastida Virgili, B., Krag, H., Klinkrad, H., Parrilla, E., Sanchez, N., Oliveira, J., and Pina, F. "DISCOS - Current status and future developments." "Sixth European Conference on Space Debris," (ESA Communications, Noordwijk, Netherlands, 2013), Aug. 2013. ISBN 978-92-9221-287-2.